

# **INTRODUCTION TO BRAIN TOPOGRAPHY**

# INTRODUCTION TO BRAIN TOPOGRAPHY

**Peter K. H. Wong**

*University of British Columbia  
and British Columbia Children's Hospital  
Vancouver, British Columbia, Canada*

With contributions by  
Hal Weinberg and Roberto Bencivenga

SPRINGER SCIENCE+BUSINESS MEDIA, LLC

Library of Congress Cataloging-in-Publication Data

---

Wong, Peter K.H.

Introduction to brain topography / Peter K.H. Wong with contributions by Hal Weinberg and Roberto Bencivenga.

p. cm.

Includes bibliographical references.

Includes index.

ISBN 978-1-4613-6653-9 ISBN 978-1-4615-3716-8 (eBook)

DOI 10.1007/978-1-4615-3716-8

1. Brain mapping. 2. Magnetoencephalography. I. Weinberg, Harold. II. Bencivenga, Roberto. III. Title.

[DNLM: 1. Brain Mapping. 2. Magnetoencephalography. WL 335 W872i]

RC386.G.B7W66 1990

612.8'22--dc20

DNLM/DLC

for Library of Congress

90-14228

CIP

---

ISBN 978-1-4613-6653-9

© 1991 Springer Science+Business Media New York  
Originally published by Plenum Press in 1991

All rights reserved

No part of this book may be reproduced, stored in a retrieval system, or transmitted in any form or by any means, electronic, mechanical, photocopying, microfilming, recording, or otherwise, without written permission from the Publisher

*This book is dedicated to  
my mother, Wai-Yuk Kwan*

# PREFACE

---

It had been difficult to find appropriate teaching material for students and newcomers to this field of brain electromagnetic topography. In part, this is due to the many disciplines involved, requiring some knowledge of the physical sciences, mathematics, neurophysiology and anatomy. It is my hope that this book will be found suitable for introducing interested workers to this exciting field. Advanced topics will not be covered, as there are many excellent texts available.

Peter K.H. Wong

# ACKNOWLEDGEMENT

---

My co-authors, Hal Weinberg and Roberto Bencivenga, for their support; Richard Harner, for all his early advice; Ernst Rodin and Gene Ramsay, for their encouragement; Wendy Cummings for her assistance; Technologists from the Department of Diagnostic Neurophysiology for collecting such excellent data; Bio-Logic Systems Corp. for permission to use some data as illustration; and all my friends and colleagues.

My wife Elke, for putting up with me throughout this presumptuous endeavour.

The manuscript was delivered in camera-ready form to the Publisher. Illustrations were created using Harvard Graphics and CorelDraw software.

# CONTENTS

---

Part 1: Fundamentals . . . . .	1
1.1 Introduction . . . . .	1
1.2 Data Acquisition . . . . .	3
Map Construction . . . . .	8
Interpolation . . . . .	12
1.3 Spatial Sampling . . . . .	16
1.4 Reference and Reference-Dependence . . . . .	20
1.5 Map Display Methods . . . . .	27
Scaling and Floating Voltage Scales . . . . .	37
Summary Maps . . . . .	37
1.6 Identification of Topographic Features . . . . .	41
1.7 Spike Mapping . . . . .	51
1.8 Post-Processing . . . . .	61
Analog Front-end . . . . .	62
Digital Filtering . . . . .	63
Reference Manipulation . . . . .	65
Statistical Mapping . . . . .	70
Global Field Power . . . . .	71
Correlation Analysis . . . . .	72
Source Localization . . . . .	73
1.9 Frequency Analysis . . . . .	76
Part 2: Source Modelling and Analysis . . . . .	81
2.1 Concepts of a Source . . . . .	81
2.2 Physical Model . . . . .	89
2.3 Inverse Solution . . . . .	96
2.4 Stability of Dipole Solutions . . . . .	102
2.5 Data Characterization . . . . .	105
Part 3: Magnetoencephalography . . . . .	113
(by Hal Weinberg)	

3.1	Instrumentation . . . . .	113
3.2	Meg Measurements and Generators . . . . .	118
	Meg Generators . . . . .	119
	Regional Generators . . . . .	123
	The Inverse Problem for MEG . . . . .	123
3.3	Spontaneous MEG Rhythms . . . . .	126
3.4	Review of MEG Studies . . . . .	129
3.5	Concerns and Outlook . . . . .	143
Part 4: Statistical Approaches . . . . .		147
(by Roberto Bencivenga)		
4.1	Introduction . . . . .	147
4.2	Assumptions and Difficulties . . . . .	149
4.3	Normative Data. . . . .	158
4.4	Statistical Comparisons . . . . .	165
4.5	Classification . . . . .	172
4.6	Exploratory vs. Confirmatory Analysis . . . . .	181
Part 5: Selected Normative Data . . . . .		185
	Flash VEP . . . . .	186
	Pattern Reversal VEP . . . . .	186
	P300 AEP . . . . .	186
	Resting EEG . . . . .	199
References . . . . .		201
Glossary . . . . .		245
Index . . . . .		253

# FIGURE LIST

---

## Part 1

- 1 - 1 Signal sampling, 4
- 1 - 2 Sampling alias, 5
- 1 - 3 Sampling precision, 6
- 1 - 4 Signal clipping, 7
- 1 - 5 Mapping EEG data, 9
- 1 - 6 Numerical map, 10
- 1 - 7 Map construction, 11
- 1 - 8 Map display, 12
- 1 - 9 Interpolation methods, 13
- 1 - 10 Interpolation effects, 15
- 1 - 11 Source location, 17
- 1 - 12 Source movement, 19
- 1 - 13 Electrode density effect, 21
- 1 - 14 Simulated topography, 23
- 1 - 15 Reference, 25
- 1 - 16 Effect of reference, 27
- 1 - 17 Spectral maps, 28
- 1 - 18 Effect of reference, 29
- 1 - 19 Bipolar electrode pairs, 31
- 1 - 20 Derivation effect, 32
- 1 - 21 Map types, 33
- 1 - 22 Grid display rotation, 34
- 1 - 23 Current flow map, 35
- 1 - 24 Hjorth derivation, 36
- 1 - 25 Display scaling, 38
- 1 - 26 Summary maps, 39
- 1 - 27a Signed summary maps, 40
- 1 - 27b Expanded time scale, 41
- 1 - 28 Map features, 42
- 1 - 29 Flash VEP, 43
- 1 - 30 Spike mapping, 44
- 1 - 31 Spike averaging, 45
- 1 - 32 Spike maps, 46
- 1 - 33 Temporal spike, 47
- 1 - 34 Digital filter, 48
- 1 - 35a Average reference, 49
- 1 - 35b Maps of 1 - 35a, 50
- 1 - 36 Source derivation, 51
- 1 - 37a Reference contamination, 52
- 1 - 37b Maps of 1 - 37a, 53
- 1 - 38 Spike foci, 55
- 1 - 39 Diffuse delta, 56
- 1 - 40 Z-statistic, 57
- 1 - 41 Z-map, 58
- 1 - 42 t-statistic map, 59
- 1 - 43 Global Field Power (GFP), 60
- 1 - 44 GFP - Flash VEP, 61
- 1 - 45 GFP - Spike, 62
- 1 - 46 Correlation, 63
- 1 - 47 Correlation map, 64
- 1 - 48 Types of correlation, 65
- 1 - 49 FFT, 66
- 1 - 50 Normal FFT, 68
- 1 - 51 Reformatted normal FFT, 69
- 1 - 52 Mu rhythm, 74
- 1 - 53 Alpha rhythm, 75
- 1 - 54 Steady-state FFT, 77
- 1 - 55 Flash VEP, 79

## Part 2

- 2 - 1 Scalp field, 82
- 2 - 2 Cortical geometry, 83
- 2 - 3 Source rotation, 84
- 2 - 4 Effect of depth, 86
- 2 - 5 Translocation, 87
- 2 - 6 Dispersion, 88
- 2 - 7 Physical head model, 90
- 2 - 8 Finite element model, 91
- 2 - 9 Coordinate system, 92
- 2 - 10 Constraints, 94

xiv Figure List

- 2 - 11 Source types, 95
- 2 - 12 Equivalent sources, 96
- 2 - 13 Source estimation, 97
- 2 - 14 Inverse solution, 99
- 2 - 15 Convergence, 100
- 2 - 16 Minima types, 102
- 2 - 17 Source approximation, 103
- 2 - 18 "Focus", 104
- 2 - 19 DLM, 105
- 2 - 20 Stability index, 106
- 2 - 21 Source fluctuation, 107
- 2 - 22 Stable solutions, 108
- 2 - 23 Map characteristics, 109
- 2 - 24 BRÉC spikes, 110

Part 3

- 3 - 1 Magnetic field strengths, 115
- 3 - 2 Gradiometer configurations, 116
- 3 - 3 60 channel MEG, 117
- 3 - 4 Shielded room, 118
- 3 - 5 Information processing, 120
- 3 - 6 Equivalent dipole, 124
- 3 - 7 Frequency analysis, 128
- 3 - 8 Magnetic field maps, 133
- 3 - 9 CNV, 135
- 3 - 10 Motor MEG potential, 139
- 3 - 11 Finger movement potentials, 141

Part 4

- 4 - 1 Normal distribution, 150
- 4 - 2 3 dimensional normal distribution, 151
- 4 - 3 Bar histogram, 152
- 4 - 4 Correlation, 153
- 4 - 5 Sample means, 155
- 4 - 6 Outlier, 158
- 4 - 7 Abnormal points, 161
- 4 - 8 Skewed distribution, 162

- 4 - 9 Box-plot, 164
- 4 - 10 Regression, 164
- 4 - 11 Regression line, 165
- 4 - 12 Principal component, 171
- 4 - 13 Overlapping populations, 173
- 4 - 14 Variance differences, 174
- 4 - 15 Linear discrimination, 175
- 4 - 16 Regional discriminants, 176
- 4 - 17 Mahalanobis distance, 177
- 4 - 18 k-nearest neighbours, 178
- 4 - 19 Classification tree, 179

Part 5

- 5 - 1a Younger normal subjects: flash VEP, 187
- 5 - 1b Older normal subjects: flash VEP, 188
- 5 - 2 P300, 189
- 5 - 3 Pattern VEP, 190
- 5 - 4 FFT maps of normal subjects
  - a) 11-15 yrs EC, 191
  - b) 16-20 yrs EC, 192
  - c) 21-30 yrs EC, 193
  - d) 31-40 yrs EC, 194
  - e) 11-15 yrs EO, 195
  - f) 16-20 yrs EO, 196
  - g) 21-30 yrs EO, 197
  - h) 31-40 yrs EO, 198

# FUNDAMENTALS

---

## 1.1 INTRODUCTION

This book provides an introduction to topographic EEG analysis. It is aimed at the practising neurophysiologist seeking an entry-level text, EEG technologists and EEG students seeking to bolster their knowledge, and the graduate student requiring help in their coursework. Material is presented and discussed at the novice and intermediate levels. Although fundamental concepts and some mathematical knowledge is covered, the emphasis is on the practical use of this new and exciting technique.

The rationale for topography is that the traditional EEG or evoked potential (EP) tracings contain information which under normal circumstances, is not appreciated by the naked eye. There is simply too much data, in a form unsuited for visual analysis. Frequency content of background EEG is one example. In this instance the solution is to apply mathematical processing by Fourier analysis, resulting in the familiar spectral plots. To discern the interrelationships between different scalp locations, one can merely arrange such plots in a manner as to mimic a head diagram, as had been demonstrated using 16 channels of EEG (Bickford 1977, 1981).

However, there are elements of the dataset which are still unrevealed: the exact location of the alpha peak, subtle asymmetries of the alpha distribution, complex phase relationships of waveforms etc. Although part of this information can be gleaned from the numerical representation, it is a laborious and non-intuitive process. It would be like trying to provide information of a city subway system by describing it entirely with words. A graphical communication of the same information (i.e., a system "map") would be more useful (Lehmann 1987).

Further argument can be applied to small time differences between channels (phase relationships). Two different epileptic foci may generate spikes that appear identical to the naked eye, due to the limited time resolution of ordinary EEG pen and paper write-out. Electronic displays with higher resolution would clearly reveal their intricate timing relationships. Coupled with suitable processing and display capabilities, a spatial-temporal analyzer for such EEG events can be implemented.

Quite apart from the display aspects of topography, there is a great selection of mathematical and statistical tools available to perform many different types of quantitative analyses. Such "post-processing" techniques cover a wide spectrum indeed. Examples include simple montage/reference reformatting and digital filtering; time-series studies, factor analysis, dynamical analysis; more advanced methods like source generator modelling/dipole localization and spatial-temporal modelling. Many of these are capable of shedding light onto hitherto hidden aspects of the data, or provide special insight by allowing interactive exploration of the datasets. It should be stated that the reader is not expected nor required to understand the intricacies of all the above techniques. They are covered within this text for the sake of completeness, and to allow the adventurous reader to wander further afield when the basics have been mastered. Indeed, it will be in one or more of these "esoteric" areas that one may find a potential solution to a current problem, or an approach that may portend a new and productive research initiative.

It is useful to view topographic analysis as a novel approach to clinical neurophysiology, to complement rather than replace the many time-proven visual analytical techniques. There are additional conceptual and technical knowledge requirements before one can skilfully extract the additional information which lies beneath the surface. To carry out clinical interpretation without adequate preparation would be inappropriate and fraught with difficulties. Likewise, to discard a new technique out of hand is equally inappropriate.

Topographic methodology includes the additional concepts of digital signal processing, computer graphics and cartography, numerical and statistical analysis, physics of electric fields, quantitative EEG and magnetoencephalography (MEG). These complex and diverse components are separated and covered in this and the

following parts. Chapters within each part are designated for specific topics, and are thus relatively short. Throughout the book, there is a noticeable profusion of illustrations. This will hopefully make an otherwise difficult topic more palatable.

For the beginner, a small selection of normal data (VEP with flash and pattern, P300, EEG with eyes open and close) for different age ranges is presented in Part 5, as a guide to some normal variations. Space limitation does not allow a full display of this data, and thus only selected maps are presented.

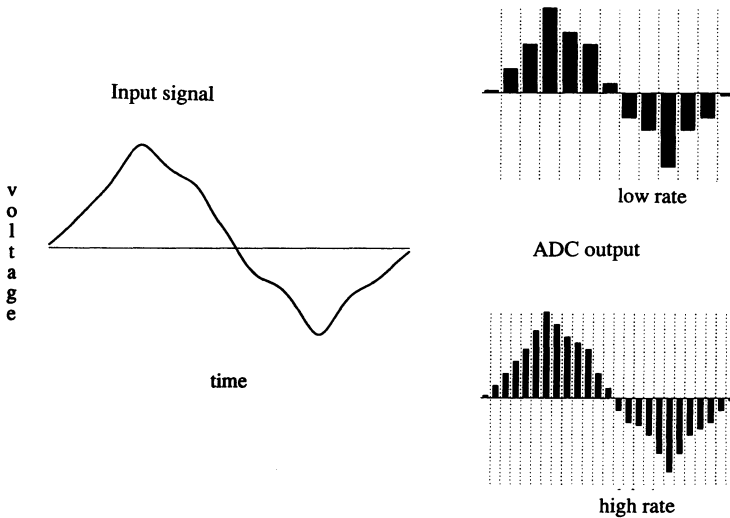
## 1.2 DATA ACQUISITION

Using an array of recording electrodes, the scalp EEG signal is amplified and filtered. It then undergoes transformation from that analog form present at the amplifier output, into information suitable for computer assimilation. This step is the analog to digital conversion (ADC). The original EEG information is now in a digital form suitable for storage in computer memory, and ready for further digital processing and display.

There are 2 important parameters which govern ADC conversion: sampling rate (Hz) and precision (bits). These will be treated separately.

Fig. 1 - 1 depicts a single channel of EEG, as present at the output of the amplifier after suitable filtering. Two sampling rates were used. The vertical lines on the right denote the times when ADC occurs. By comparing this rate to the number of perturbations present in the signal in a given time window (say 1 sec.), one can appreciate that the first rate (top right) is low, and the digitized result is a crude representation of the original signal. The higher sampling rate (bottom right) produced a much smoother output, which was able to capture all the perturbations, or follow the changes of the signal faithfully. This "high fidelity" characteristic of digitization is important because it dictates the amount of temporal precision which can be achieved.

Inadequate sampling rate can occur if the frequency content of the signal is too high in relation to the sampling rate. Theoretically,

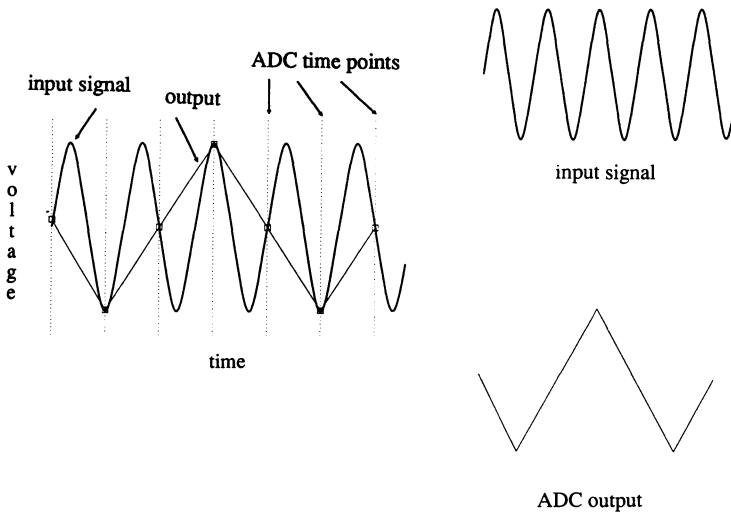


1-1: Signal digitization. Left: input signal; right: output signals for different sampling rates (top=low rate, bottom=high rate).

the minimum sampling rate should be twice the highest frequency component contained in the signal. In practice, as the low-pass filters generally used during EEG amplification have a gradual roll-off in the frequency response curve, it is safer to sample at a minimum of 3 or 4 times the cut-off setting for the low-pass filter.

To illustrate the problems with inadequate sampling rate, Fig. 1 - 2 shows an input signal at one frequency being digitized into an output which contains some slower activity, which is obviously an artifact created by the sampling process. Such "alias" error is insidious and permanent, because it cannot be detected after ADC is completed, nor can it be removed. Along the same lines, an EEG input with high frequency beta may then possibly become contaminated with delta activity.

ADC precision is expressed as the number of "bits" which is used to represent any given voltage level. As Table 1 indicates, a precision of 8 bits means that there can be 256 such levels, while 10 bits means 1024 levels are available. Tied closely to this are the related parameters of dynamic range (through which the signal can vary without "clipping" or saturation distortions), and the minimum



1-2: Sampling alias. The input signal is shown at the top right and on the left composite tracing. The dotted vertical lines are the times when ADC at a slow rate occurred, with the output a seemingly triangular waveform.

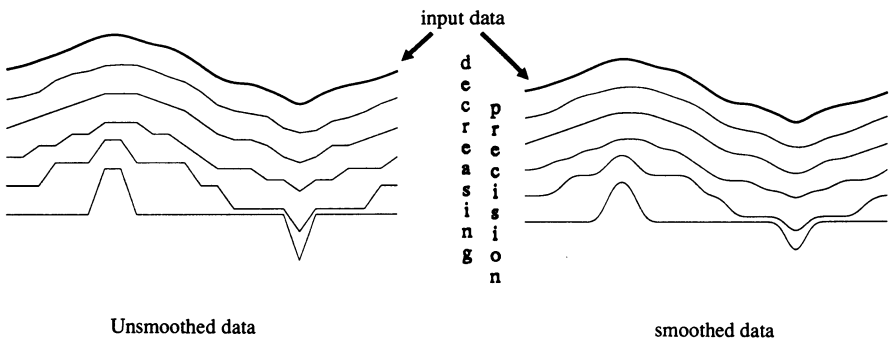
ADC voltage accuracy (ADC step size or "error"). If 8 bits were used to represent a range of 512  $\mu\text{V}$  (or  $\pm 256 \mu\text{V}$ ), then the absolute ADC voltage error is 2  $\mu\text{V}$ , as any variation can only be in steps of 2  $\mu\text{V}$ . However if a range of  $\pm 1024 \mu\text{V}$  is desired, then for the same ADC precision, the step size is 8  $\mu\text{V}$ . If the requirements for the recording is such that this step size is unacceptably large, then the only alternative would be to increase the number of bits used.

Fig. 1 - 3 shows the effect of sampling at different precision. Here the input tracing is being represented by 6 bits, and shows the tracings obtained with decreasing precision. At the minimum precision of 1 bit (bottom tracing) there are only 2 voltage levels: zero or maximum! However, the poor quality of the tracings may be hidden by the simple act of filtering, as may be done by software. As the right side of Fig. 1 - 3 shows, the smoothed tracings merely look better, but do not approximate more the input signal any better.

To put things in perspective, EEG spikes are of the order of 100  $\mu\text{V}$ , while evoked potential waves can be from a fraction of a microvolt to 30 or 40  $\mu\text{V}$ . In practice, it is useful to know that the ADC precision is usually determined by the electronic hardware

Table 1: Relationship between ADC precision and digitized data results.

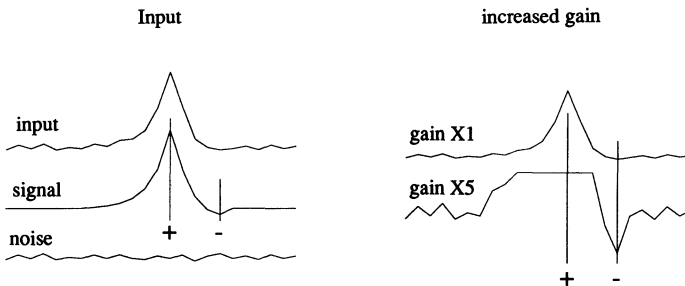
# of bits	# levels	step size	range
8	256	1 uV	+/- 128 uV
		2	+/- 256
		4	+/- 512
10	1024	1	+/- 512
		2	+/- 1024
		4	+/- 2048
12	4096	1	+/- 2048
		2	+/- 4096



1-3: ADC precision. The input data is shown in bold line at the top, with decreasing levels of sampling precision (from 6 bits at input, to 1 bit for the lowest tracing). The visual effect of smoothing of the same data (right) is that of an artificially higher precision.

selected, so that the user has no choice. Based on this pre-determined precision, the user must make a compromise between step size and dynamic range. Again, the easiest way is to think in terms of the electrical short-circuit noise of the amplifier system. It is not useful to have the ADC minimum voltage step size much smaller than this noise value. So one selects the step size at the value closest to the amplifier noise. From this point on, the dynamic range is effectively determined.

Difficulty arises if this dynamic range is too small for the signal amplitude range. Then one must either accept a coarser ADC step size with the accompanying "choppy" output, or use hardware that can provide greater ADC precision, thus allowing the same voltage accuracy but able to accommodate a greater input voltage range. Fig. 1 - 4 shows the influence which amplifier gain has on the dynamic range and voltage accuracy. The input consists of the sum of signal and noise. At a low gain, there is no saturation (or clipping), but the low voltage details are missing. At high gain (x5) these details are clear, but clipping has occurred. Such a compromise between gain and fidelity may be avoided if the original data had been sampled at a higher precision, effectively raising the clipping threshold. Like alias error, saturation error is permanent, with no recourse for data recovery once sampling is completed. If a fixed precision ADC is used, the only recourse is for the amplifier gain to be lowered until the dynamic range is sufficient to avoid clipping.



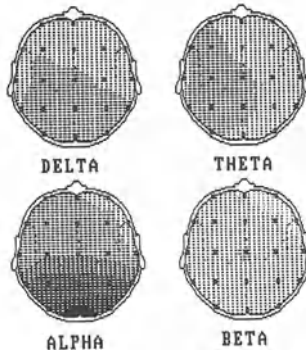
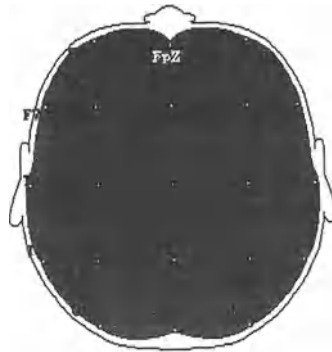
1-4: Amplifier gain and clipping. Left: the input tracing (top) consists of signal (middle) and noise (bottom). Right: the effect of increasing the gain: the bottom tracing (x 5) shows clipping of the positive peak, while the smaller noise ripples are enhanced.

## Map construction

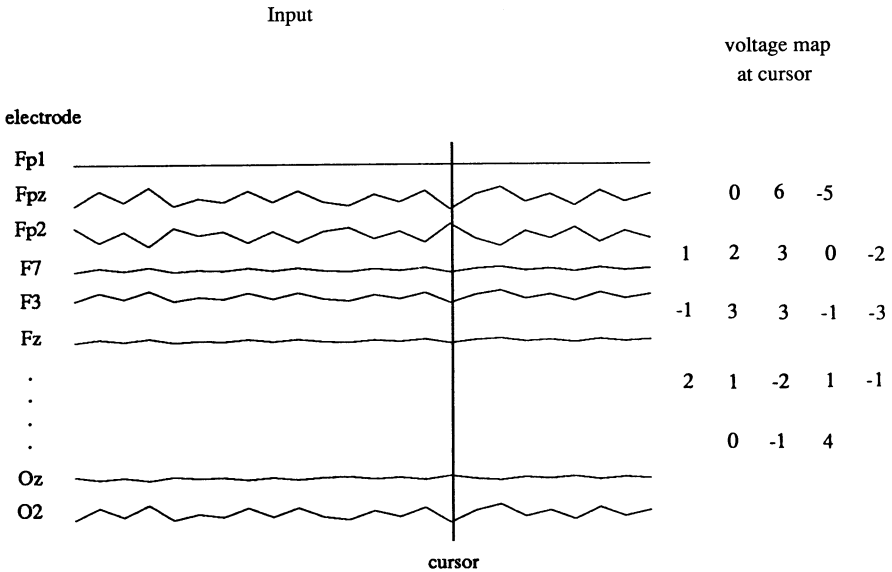
Let us assume that a set of scalp electrodes applied according to the International 10 - 20 System (henceforth referred to as 10 - 20 system) had been used to record an EEG signal, and that adequate digitization had been carried out. The resulting data is in the form of individual tracings which represent voltage variation with time, or a "time series". One can display these tracings in anatomically meaningful arrangements, by arranging the tracings more or less in the respective head locations. To be able to fully appreciate at a glance all the subtleties of the spatial information present, a totally different form of data display is required. Such a display must convey the anatomic or spatial element (i.e., based on some sort of a head diagram), and also the amplitude information pertaining to the potential field of interest. Fig. 1 - 5 illustrates how the common example of frequency power display can be adapted, showing the topographic features of the various frequency bands. No ideal method exists that can allow all the temporal and spatial information of a segment of EEG data to be displayed in one diagram. By limiting each individual display to a given time window, and by allowing a successive series of such displays, useful topographic displays can be constructed, based on the idea that a pictorial representation of the instantaneous potential field can convey useful information.

A rudimentary "map" can be constructed merely as the arrangement of the voltage amplitude at one time instant, as given in Fig. 1 - 6. This is inconvenient for visual analysis, as all 19 voltage values in each "frame" must be completely scanned and remembered before the voltage field which it depicts can be appreciated. Such a process would be extremely tedious. To simplify this, each frame is transformed into voltage-coded maps. This is simply a "colouring" process where a set of colours (or shades of grey) are used to convey voltage. The dynamic range is equally divided into the same number of voltage bins, so that actual voltage values falling within a given colour's bin is assigned that colour. By a process of "pseudo colouring", the purely numerical map is transformed into a colour display. This same approach is used to provide colour to originally black and white motion pictures. Fig. 1 - 7 illustrates the process of map construction.

	<b>Fp1</b>	<b>Fpz</b>	<b>Fp2</b>	
<b>F7</b>	<b>F3</b>	<b>Fz</b>	<b>F4</b>	<b>F8</b>
<b>T3</b>	<b>C3</b>	<b>Cz</b>	<b>C4</b>	<b>T4</b>
<b>T5</b>	<b>P3</b>	<b>Pz</b>	<b>P4</b>	<b>T6</b>
	<b>O1</b>	<b>Oz</b>	<b>O2</b>	



1-5: Map construction. The electrode array (top) is superimposed onto a head diagram (middle). By assigning appropriate values at each of the electrode positions, meaningful topographic displays result (spectral band maps - bottom).



1-6: Numerical display. The voltage readings at all channels at any given instant (cursor on the left) is displayed anatomically (right).

A single map may represent the magnitude of the instantaneous potential field for a single time point, or some mathematical representation of the voltage field during a given time window (e.g., mean voltage). An illustration using the alpha rhythm can be seen in Fig. 1 - 8. The colour scale used here is such that black and white represent maximum and minimum amplitudes respectively, while the grey shades in between represent all other intervening amplitudes (i.e., a unipolar scale). The occipital prominence is obvious, with a tapering-off of the field towards the anterior head. If sequential maps are shown, there would be a pattern of fluctuation between high and low magnitudes occurring at the alpha frequency of 10 Hz.

At the coarser time windows of 1 sec. used here, the details of how the field changes with time is lost, and all that remains is the overall pattern of occipital prominence. This happens since the original data is a persistent occipital dominant alpha rhythm, with no fluctuation or change over the time period under study. The maps for the 1 sec. windows thus depict the averaged activity over the